



Single and repeated dose toxicity of mesoporous hollow silica nanoparticles in intravenously exposed mice

Tianlong Liu ^a, Linlin Li ^a, Xu Teng ^b, Xinglu Huang ^a, Huiyu Liu ^a, Dong Chen ^a, Jun Ren ^a, Junqi He ^b, Fangqiong Tang ^{a,*}

^a Laboratory of Controllable Preparation and Application of Nanomaterials, Technical Institute of Physics and Chemistry, Chinese Academy of Sciences, No.2 Beiyitiao Zhongguancun, Beijing 100190, China

^b Department of Biochemistry and Molecular, School of Basic Medical Sciences, Capital Medical University, Beijing 100069, China

ARTICLE INFO

Article history:

Received 1 October 2010

Accepted 15 October 2010

Available online 19 November 2010

Keywords:

Mesoporous hollow silica

Biocompatibility

Biodistribution

Clearance

Repeated dose toxicity

ABSTRACT

Mesoporous hollow silica nanoparticles (MHSNs) are emerging as one of the new and promising nanomaterials for biomedical applications, but the biocompatibility of MHSNs *in vivo* has received little attention. In the present study, the systematic single and repeated dose toxicity, biodistribution and clearance of MHSNs *in vivo* were demonstrated after intravenous injection in mice. For single dose toxicity, lethal dose 50 (LD₅₀) of 110 nm MHSNs was higher than 1000 mg/kg. Further repeated dose toxicity studies indicated no death was observed when mice were exposed to MHSNs at 20, 40 and 80 mg/kg by continuous intravenous administration for 14 days. These results suggest low toxicity of MHSNs when intravenous injection at single dose or repeated administrations. ICP–OES and TEM results show that the MHSNs mainly accumulate in mononuclear phagocytic cells in liver and spleen. In addition, these particles could be excreted from the body and the entire clearance time of the particles should be over 4 weeks. These findings would be useful for future development of nanotechnology-based drug delivery system and other biomedical applications.

© 2010 Elsevier Ltd. All rights reserved.

1. Introduction

The application of nanoparticles (NP) in the field of drug delivery has attracted much attention in recent decades. However, before these nanomaterial can be safely applied in a clinical setting, their biocompatibility, biodistribution and clearance needs to be carefully assessed [1,2]. In recent years, much research has been carried out to assess toxicity of NP, but studies are fragmented, and very often contradictory. Furthermore, a majority of nanotoxicity researches have focused on cell culture systems; however, the data from these studies could be misleading and will require verification from animal experiments. *In vivo* systems are extremely complicated and the interactions of the nanostructures with biological components, such as proteins and cells, could lead to unique biodistribution, clearance, immune response, and metabolism [3]. In addition, due to the great differences between nanomaterials, the generalization of potential toxicological effects is extremely difficult.

Progresses in mesoporous silica nanomaterials (MSN) over the last decade offered exciting opportunities in the development of drug delivery systems which meet the need for better control of drug administration [4–8]. However, the drug storage capacity for the conventional mesoporous materials is relatively low, and also the irregular bulk morphology is not perfect for drug delivery [9]. To overcome these problems, one strategy is to synthesize mesoporous hollow silica nanoparticles (MHSNs) with penetrating pore channels from outside to the inner hollow capacity. Studies on MHSNs indicate that they have a sustained release property and a much higher drug loading capacity than conventional mesoporous silica, such as MCM-41 and SBA-15 [10,11]. However, for synthesizing nanomaterials with hollow structure, the synthesis processes are often tedious and they are also difficult to be scaled up. And, dispersibility remains a problem in many synthesis processes, especially after drying. Recently, we reported a flexible, scalable and robust method to prepare rattle-type mesoporous silica hollow spheres [12]. Compared with current methods used for preparing rattle-type nanomaterials, our selective etching strategy as well has many obvious advantages: significant monodispersion, large scale and general method to fabricate functional nanoparticles. MHSNs are emerging as a new and promising class of

* Corresponding author. Tel./fax: +86 10 82543521.

E-mail address: tangfq@mail.ipc.ac.cn (F. Tang).

nanoparticles that developed for drug delivery system due to their special structure and functions.

Similar to other NPs, the concerns on the biosafety impacts caused by MHSNs are also being increase [13–15]. Several studies have demonstrated that the biocompatibility of MHSNs on a variety of cell types *in vitro* is fairly high [16–19]. However, the low cytotoxicity *in vitro* offers no guarantee on the desired high biocompatibility *in vivo*. Furthermore, most of the toxicology studies of NPs *in vivo* so far were mainly focused on the effects of NPs that enter the body accidentally [20–22]. There has been much less research on the toxicology of NPs that are used for biomedical applications, such as drug delivery or imaging, in which the NPs are deliberately placed in the body. To the best of our knowledge, few *in vivo* studies exist on the toxicity of mesoporous silica particles, especially the repeated dose toxicity.

Here, we examine the toxicity of mesoporous materials with hollow structure using rattle-type MHSNs as a model particle, specifically as drug delivery vehicles entered the blood stream. Rattle-type MHSNs was synthesized via a simple, scalable method. These type particles have hollow structure, mesopores, controllable size, and narrow size distribution. Its single and repeated dose toxicity was evaluated by intravenous injection for one time and for 14 days, respectively. Clearance of circulating nanoparticles during systemic delivery is a critical issue for nanoparticles drug delivery systems. It is necessary to understand the factors affecting particle biodistribution and blood circulation half-life. Therefore, we also examine biodistributions in different organs and clearance of MHSNs in mice.

2. Materials and methods

2.1. Materials

Tetraethylorthosilane (TEOS), N-[3-(trimethoxysilyl)propyl]ethylenediamine (TSD), 3-aminopropyltrimethoxysilane (APTMS), hydrofluoric acid (HF) were obtained from Beijing Chemical Reagents Company (China). Fluorescein isothiocyanate (FITC), potassium EDTA, hematoxylin and eosin were obtained from Sigma.

2.2. Fabrication and characterization of MHSNs

MHSNs were synthesized as described previously [12]. Morphology and structure of the resulting MHSNs were observed with a JEOL-200CX transmission electron microscope (TEM).

2.3. Fluorescent labeling of MHSNs

Fluorescein isothiocyanate (FITC) was doped into the core of the MHSNs via coupling with 3-aminopropyltrimethoxysilane (APTMS) and co-condensing with tetraethylorthosilane (TEOS) in the formation of the core of hybrid solid silica spheres (HSSs). The number of FITC molecules conjugated to MHSNs was determined by measuring the fluorescence intensity of a diluted sample of FITC MHSNs at an emission wavelength of 520 nm and then comparing these values to a standard curve prepared using various concentrations of FITC.

2.4. Animals

All animal experiments were performed in compliance with the local ethics committee. Both sexes ICR mice (provided by Weitonglhua experimental animal Co., Ltd), aged 6–8 weeks, were used in the experiments. Every five same sex mice were housed in stainless steel cages containing sterile paddy husk as bedding in ventilated animal rooms. They were acclimated in the controlled environment (temperature: 22 ± 1 °C; humidity: $60 \pm 10\%$ and light: 12 h light/dark cycle) with free access to water and a commercial laboratory complete food.

2.5. Single dose toxicity

In the dose probing study, ten ICR mice were used at the high dose of MHSN (Fig. 2A). For Single dose toxicology research of MHSNs, a series of doses were set based on pilot study as the above described (Fig. 2B). Intravenous injections of MHSNs suspension in physiological saline were conducted through the mouse tail vein. Intravenous injections of sterile physiological saline were also given to mice as controls. Mortality was recorded and the bodies were sent for an immediate necropsy.

2.6. Repeated dose toxicity

For further repeated dose toxicity study, mice were dosed at different levels for 14 days (Fig. 2C). After injection, ration, body weight and clinic manifestation were recorded at the time points according to the regulation. The symptom and mortality were observed and recorded carefully throughout the entire study. At the end of experiment, all animals were sacrificed.

2.7. Hematology analysis and blood biochemical assay

Blood was drawn for hematology analysis (potassium EDTA collection tube) using a standard saphenous vein blood collection technique. We selected the following standard hematology markers for analysis: red blood cell count, hemoglobin, hematocrit, mean corpuscular volume, mean corpuscular hemoglobin, mean corpuscular hemoglobin concentration, platelet count, and white blood cell count. Blood samples which collected via the ocular vein (about 0.8–1 ml each mouse) were centrifuged twice at 3000 rpm for 10 min in order to separate serum. In the present study, liver function was evaluated with serum levels of total bilirubin levels (TBIL), alanine aminotransferase (ALT), aspartate aminotransferase (AST) and alkaline phosphatase (ALP). Nephrotoxicity was determined by blood urea nitrogen (BUN) and creatinine (Cr). The enzyme of lactate dehydrogenase (LDH) was assayed for evaluating cardiac damage. Albumin (ALB) was assayed as one parameter of damage of tissue or inflammation. These parameters were all assayed using a Biochemical Autoanalyzer (Type 7170, Hitachi, Japan).

2.8. Coefficients of liver, spleen and kidneys

The tissues and organs, such as heart, liver, spleen, kidneys, lung, brain, and testicle were excised and weighed accurately. The coefficients of liver, kidneys, and spleen to body weight were calculated as the ratio of tissues (wet weight, mg) to body weight (g).

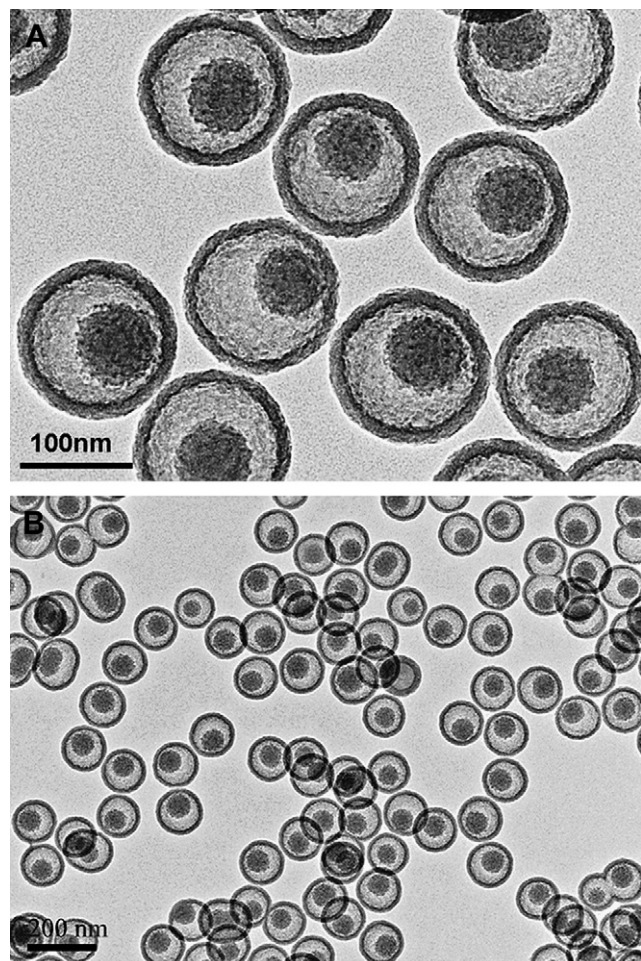


Fig. 1. TEM images of MHSN in different dispersants. Well-defined size and shape of 110 nm MHSN (core = 53 nm and shell = 13 nm) showed well monodispersity in pure water (A) and saline (B), respectively.

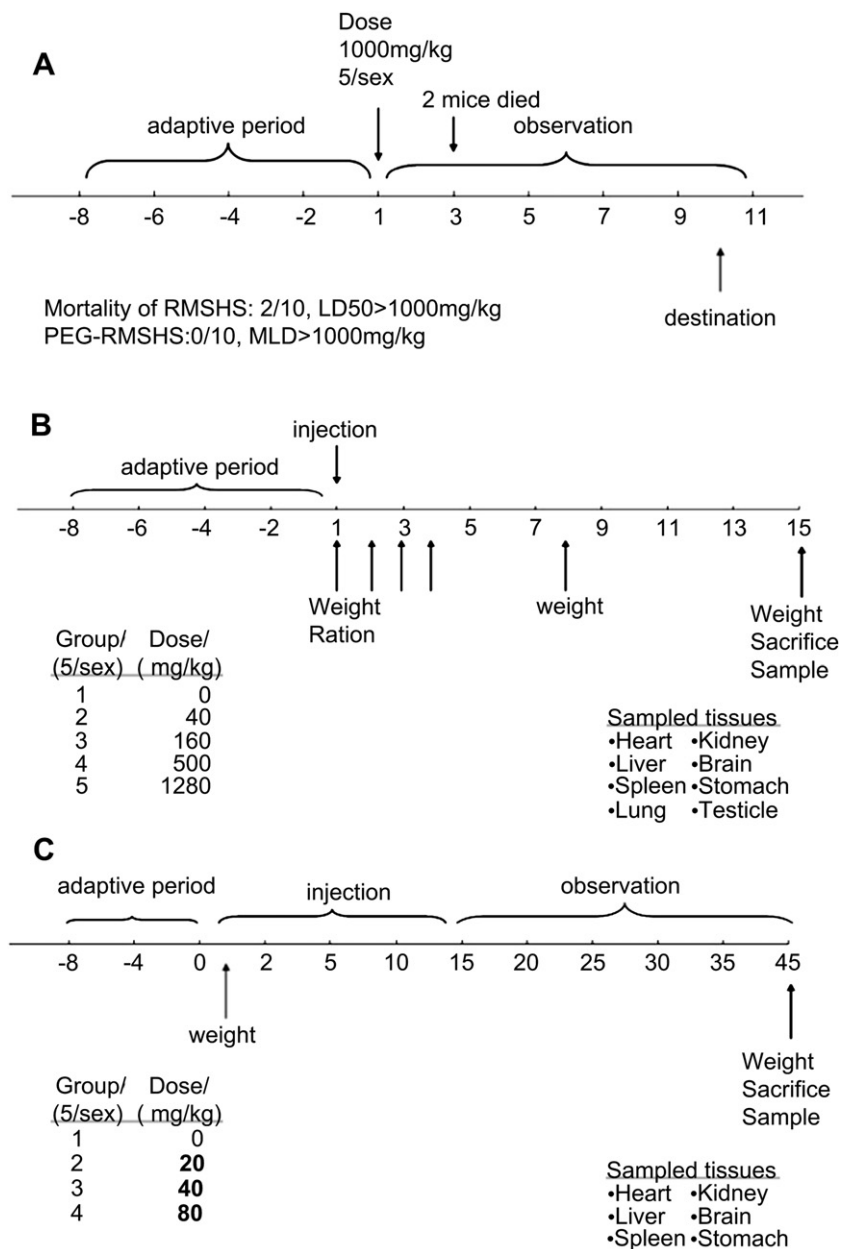


Fig. 2. A) Design of pilot study of MHSN in ICR mice for dose selection, B) Experimental design of single dose toxicity study of MHSN in mice, C) Experimental design of repeated dose toxicity study of MHSN in mice.

2.9. Histopathological examinations

Tissues recovered from the necropsy were fixed in 10% formalin, embedded in paraffin, sectioned, and stained with hematoxylin and eosin (HE) for histological examination using standard techniques. After hematoxylineosin staining, the slides were observed and photos were taken using optical microscope (Olympus X71, Japan). All the identity and analysis of the pathology slides were blind to the pathologist.

2.10. TEM imaging of tissues

For electron microscopy, liver and spleen tissues were excised at 24 h after MHSNs injected at 80 mg/kg and immediately fixed in 3% glutaraldehyde overnight, then the samples were treated according to the general protocols for TEM study. The ultrathin sections (60 nm) were stained with lead citrate and uranyl acetate. The sections were viewed on a Hitachi H-7650 TEM, operating at 80 kV. All the identity and analysis of the ultrathin section were blind to the pathologist.

2.11. Fluorescent localization of MHSNs

The animals treated by FITC-MHSNs at 80 mg/kg were killed after injection for 24 h. The tissues, such as heart, liver, spleen, kidneys, lung, brain, were excised and

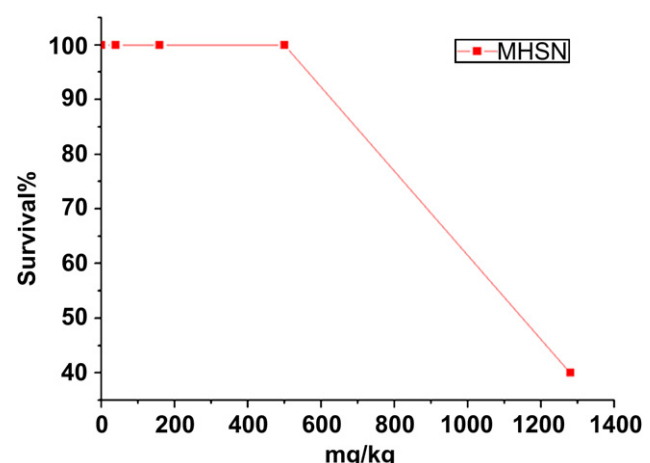


Fig. 3. Percentage survival of mice injected intravenously with 0.2 ml of MHSN suspension in saline (n = 10).

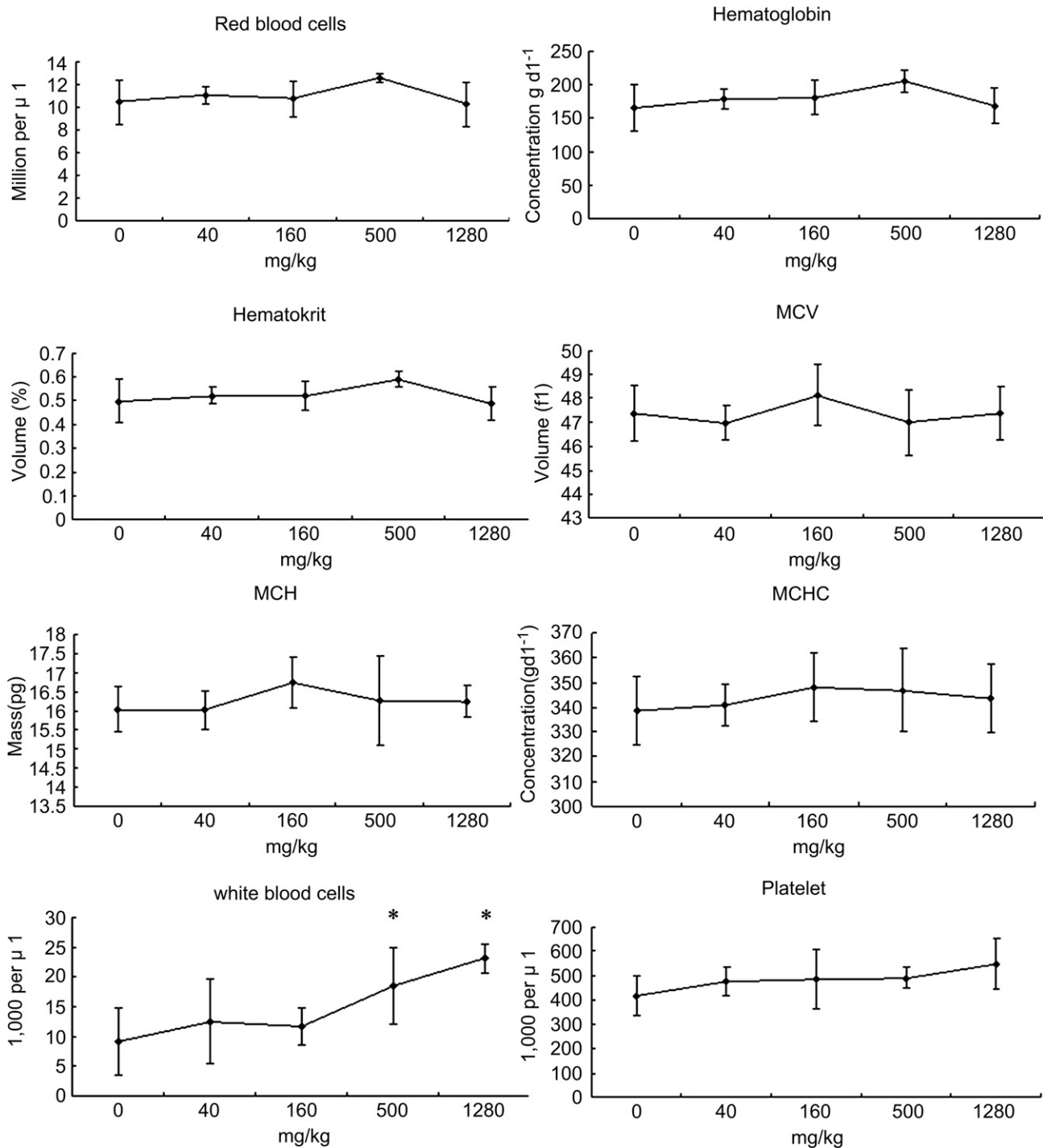


Fig. 4. Complete blood counts of ICR mice following injection of MHSN. Mean and standard deviation of red blood cell numbers, hemoglobin concentration, hematocrit, mean corpuscular volume (MCV), mean corpuscular hemoglobin (MCH), mean corpuscular hemoglobin concentration (MCHC), white blood cells or platelet of ICR mice ($n = 10$). No statistically significant changes were observed between groups, with the exception of significant spread in white blood cell counts in 500 and 1280 mg/kg dose group of MHSN particles (*denotes statistical significance for the comparison of control, $*p < 0.05$).

frozen at -80°C . Frozen sections were made and the images were observed with Nikon fluorescence microscope (Nikon Eclipse Ti-S, CCD: Ri1).

2.12. Silicon content analysis

For *in vivo* biodistribution studies, the mice injected at 80 mg/kg dose were sacrificed after injection for 1 day, 1 week and 4 weeks after injection. And brain, heart, kidney, liver, lung and spleen were collected. To determine the silicon content in the tissues, the wet samples were weighed, digested with nitric acid by heating

and then analyzed for silicon content using inductively coupled plasma-Optical Emission Spectrometer (ICP-OES, VARIAN VISTA-MPX, US).

2.13. Statistics

Results were expressed as mean \pm standard deviation (S.D.). Multigroup comparisons of the means were carried out by one-way analysis of variance (ANOVA) test using SPSS 14.0 (SPSS Inc., Chicago, IL). The statistical significance for all tests was set at $p < 0.05$.

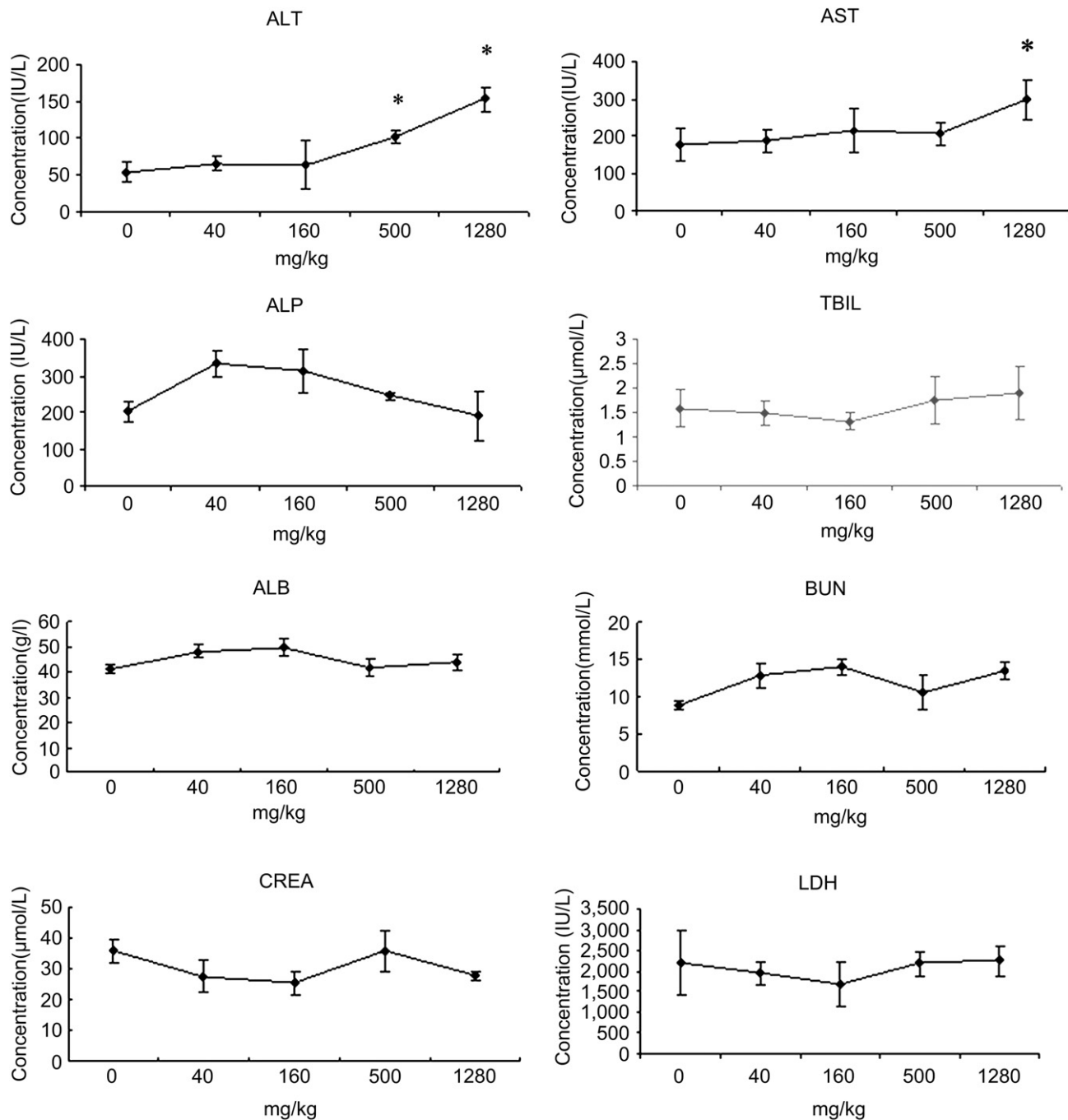


Fig. 5. Clinical Chemistry indexes of ICR mice following injection of MHSN. Mean and standard deviation of aspartate aminotransferase (AST), alanine aminotransferase (ALT), alkaline phosphatase (ALP), total bilirubin (TBIL), albumin (ALB), Creatinine (CREA), blood urea nitrogen (BUN) or lactate dehydrogenase (LDH) of ICR mice ($n = 10$ per group). The serum ALT or AST level of the 500 and 1280 mg/kg MHSN groups increased significantly ($p < 0.05$) comparing with control. (*)denotes statistical significance for the comparison of control, $*p < 0.05$.

3. Results

3.1. Preparation and characterization of MHSNs

MHSNs had well monodispersion in deionized water (Fig. 1A) and physiological saline (Fig. 1B). The average size of the silica particles was about 110 nm by Zetasizer 3000HSA (Malvern) at 25 °C. MHSNs was sterilized by UV irradiation for 2 h, then suspended in sterile physiological saline and sonicated for 15 min before being loaded into 1 ml syringes under sterile conditions. An endotoxin assay showed that there was no detectable gram

negative endotoxin on any of the four particle types at a concentration of 1 mg/ml (the detection limit was less than 0.1 EU/ml).

3.2. Single dose toxicity of MHSNs

3.2.1. Single dose toxicity and LD_{50} in vivo

In the dose probing study, only 2 mice were injected with MHSNs died (2/10) at 1000 mg/kg (Fig. 2A), which indicated that lethal dose 50 (LD_{50}) of MHSNs was higher than 1000 mg/kg. To determine detailed single dose toxicity of MHSNs, experimental animals were dosed at different levels according to the preliminary experimental

results (Fig. 2B). After exposure, the mortality in each dose group was observed through the entire experiment. In the low dose groups (40, 160 and 500 mg/kg), no death and unusual behaviors were observed, including vocalizations, laboured breathing, difficulties moving, hunching or unusual interactions with cage mates (Table S1). While the mice treated with MHSNs at 1280 mg/kg obviously

appeared changes such as loss of appetite, lose weight, passive behavior, and 6 mice died in 3 days (Table S2 and Fig. 3).

3.2.2. Coefficients of liver, spleen and kidneys

The coefficients of liver and spleen significantly elevated after injection at 500 and 1280 mg/kg of MHSNs compared with the control

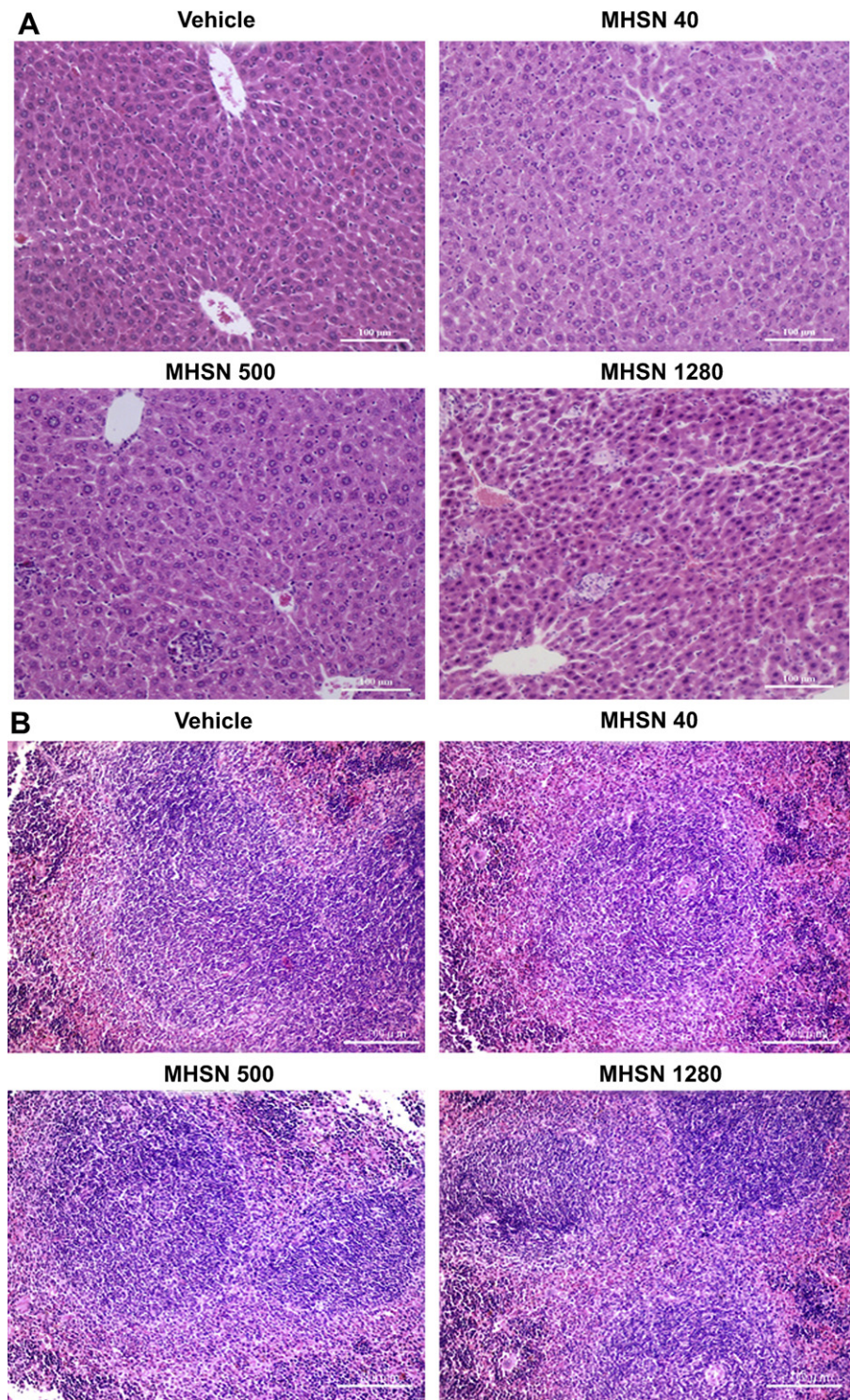


Fig. 6. Histological analyses of tissues in silica particle-treated mice. MHSNs were intravenously administered to mice at vehicle, 40 (MHSN40), 500 (MHSN500) and 1280 (MHSN1280) mg/kg, respectively. Histological section of liver (A) and spleen (B) stained with H&E. Data are representative of at least 8 mice. The scale bar is 100 μ m.

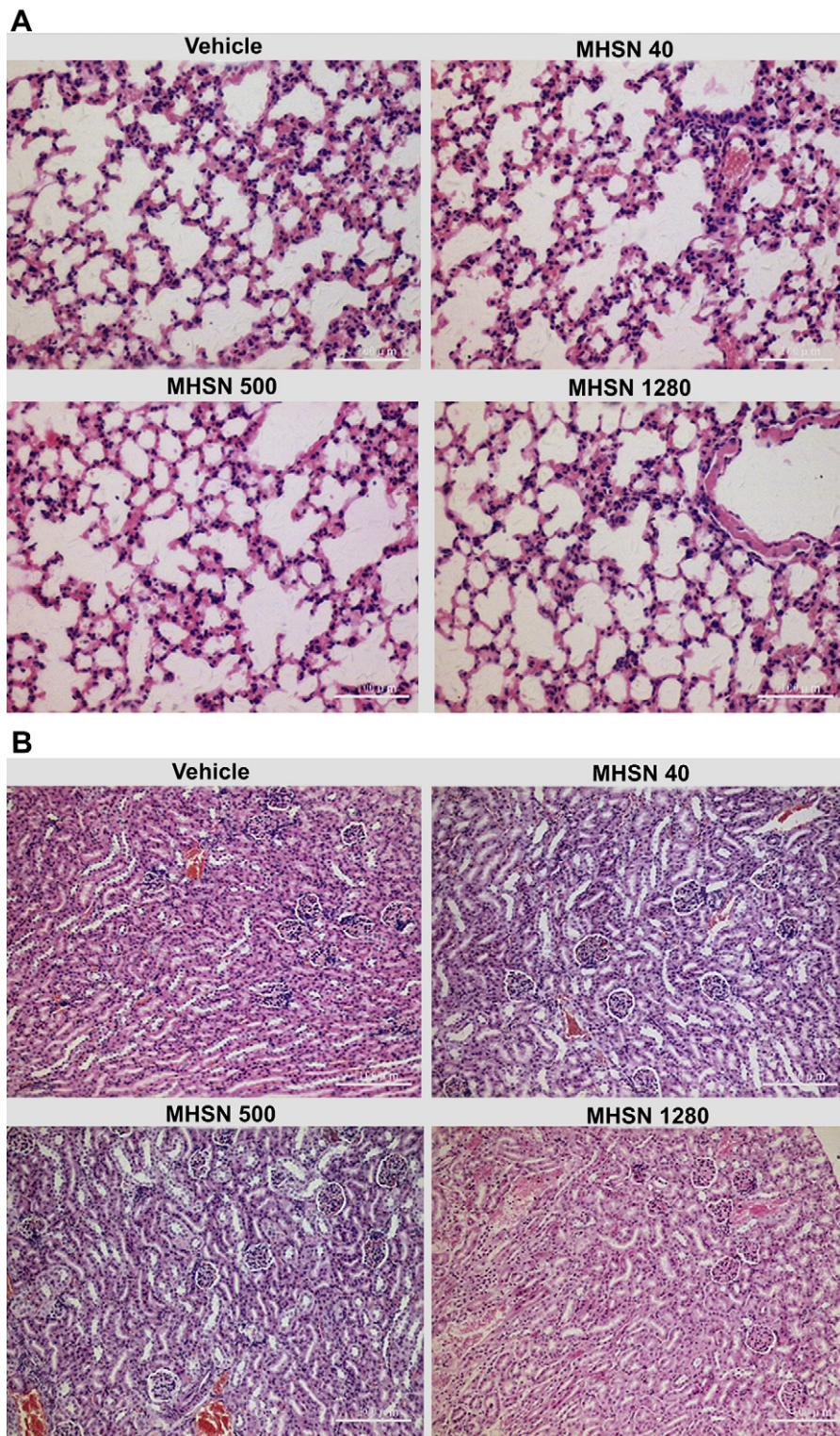


Fig. 7. Histological analyses of tissues in MHSNs treated mice. MHSNs were intravenously administered to mice at vehicle, 40 (MHSN40), 500 (MHSN500) and 1280 (MHSN1280) mg/kg, respectively. Histological section of lung (A), and kidney (B) stained with H&E. Data are representative of at least 8 mice. The scale bar is 100 μ m.

group ($p < 0.05$) (Table S2). No significant changes were observed in coefficients indexes after administration of MHSN at other doses.

3.2.3. Hematology and blood biochemical assay

Representative hematology results indicated that measured factors were within normal ranges and there were significantly not

difference between groups of low dose (40, 160 mg/kg) and control (Fig. 4). Animals treated with higher dose (500, 1280 mg/kg) showed significant spread in white blood cell counts ($p < 0.05$) (Fig. 4). The serum ALT or AST levels of 500 and 1280 mg/kg groups increased significantly ($p < 0.05$) compared with the control group. The ALT or AST levels changed from all treatment groups revealed

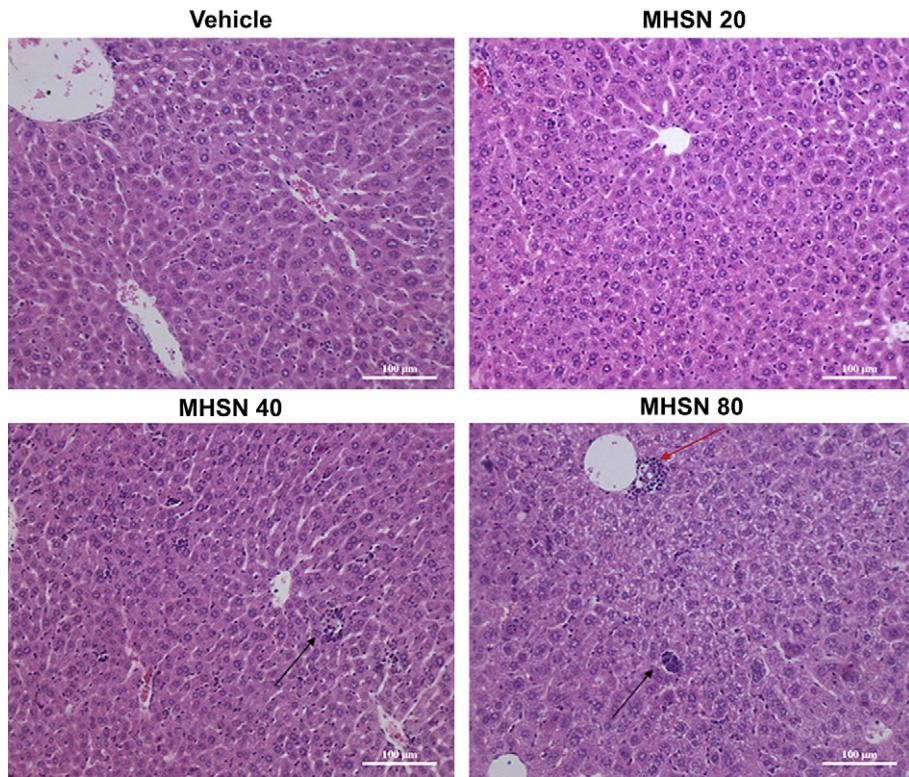


Fig. 8. Micromorphological change of liver after injected at 20 (MHSN20), 40 (MHSN40) and 80 (MHSN80) mg/kg by continuous intravenous administration for 14 days. Histological section of vehicle (A), 20 (B), 40 (C) and 80 mg/kg (D) stained with H&E. Data are representative of at least 8 mice. The scale bar is 100 μ m.

a dose-dependent manner after intravenous injection. No significant changes were observed in other biochemical indexes after administration of MHSN at all doses (Fig. 5).

3.2.4. Pathological changes in mice

MHSN particles would not induce any changes in appearance and micro morphology of liver at 40 and 160 mg/kg (Fig. 6A). In contrast, lymphocytic infiltration, microgranulation and degenerative necrosis of hepatocytes were obviously observed at 500 and 1280 mg/kg (Fig. 6A). The pathological changes of the main viscera and their severeness observed from all treatment groups revealed a dose-dependent manner after intravenous injection (Table S3). Liver was the mainly involved targeting organ of MHSN treated at high dose and displayed as degeneration, lymphocyte infiltration and necrosis. Although coefficients of spleen significantly elevated after injection at 500 and 1280 mg/kg of MHSNs, spleen samples showed no significant changes in micro morphology of the lymphoid follicles and in the size of the red pulp after injection of MHSNs at all doses (Fig. 6B). Kidney and lung samples also showed no remarkable change in the morphology (Fig. 7A and B).

3.3. Repeated dose toxicity of MHSNs

3.3.1. Mortality and clinic manifestation

For further repeated administration toxicity study, mice were dosed at different levels (Fig. 2C). Animals received continuous intravenous administration for 14 days and observed 1 month. No animals died when mice exposed to nanoparticles at 20, 40 and 80 mg/kg. In the entire study period, no unusual behaviors were observed, including vocalizations, laboured breathing, difficulties moving, hunching or unusual interactions with cage mates (Table S4).

3.3.2. Coefficients of liver, spleen and kidneys

After 45 days, the mice were sacrificed and the weight of body and various tissues/organs were collected. No obvious differences were found in the body weight of four groups. The coefficients of liver and spleen significantly elevated after injection at 80 mg/kg of MHSNs compared with the control group ($p < 0.05$). The significant difference was not observed in the kidneys of this dose. Coefficients of liver, spleen and kidneys at 20 and 40 mg/kg showed no remarkable change after administration of MHSNs (Table S4).

3.3.3. Pathological changes in mice

We found no toxicity in any of organs in MHSNs injected mice at 20 mg/kg, and no abnormalities in the spleen, kidney and lung in MHSNs injected mice at 40, 80 mg/kg. However, lymphocytic infiltration and microgranulation of hepatocytes in the liver were observed in MHSNs injected mice at 40 and 80 mg/kg, suggesting that MHSNs at high dose was toxic to the hepar (Fig. 8).

3.3.4. Blood biochemical assay

The observations from the pathological examinations indicate that liver is the target organ for MHSNs via the intravenously exposure route. Hence, blood biochemical parameters that reflect the hepatic functions were further investigated. Serum ALT or AST levels were increased with MHSNs administration at 80 mg/kg, while no increase was observed at 20 and 40 mg/kg. There were no significant changes for others biochemical indexes after administration of MHSNs (Fig. 9). The liver pathological changes and blood biochemical indexes revealed a dose-dependent manner after MHSNs injection. So no observed adverse effect level (NOAEL) of MHSNs was 20 mg/kg by continuous intravenous administration for 14 days.

3.4. Biodistribution *in vivo*

3.4.1. Fluorescent and ultrastructure localization

To investigate the fate of particles *in vivo*, MHSN was injected intravenously at 80 mg/kg in mice. Fluorescent and ultrastructure localization indicated that MHSN was recognized and internalized by resident macrophages in liver and spleen. The fluorescent substance mainly localized in the marginal zone of spleen and hepatic sinus of liver, respectively (Fig. S1, green fluorescence). To further confirm this phenomenon, the uptake of nanostructures by macrophage was visualized by TEM observation. MHSNs persist in membrane-enclosed vesicles called lysosomes (Fig. 10) in the liver and spleen macrophages without unnormal changes of ultrastructure. The particle size of MHSN trapped mainly in the liver and spleen was virtually the same as *in vitro*.

3.4.2. Silicon content analysis

Inductively coupled plasma-Optical Emission Spectrometer (ICP-OES) analysis reveals that the changes of silicon contents varied from tissue to tissue. Silicon levels in liver and spleen peaked at 24 h and then declined over 4 weeks. Other tissues also experienced increased silicon contents 24 h after the MHSN injection, but this increase was relatively smaller in heart, lung, and kidney than liver and spleen tissues. About 85% of the injected MHSN localized in spleen and liver at 24 h and then reduced to about 60% after 1 week. At 4 weeks following particle injection, silicon levels in the liver corresponded to 7% of the injected dose and 41% in the spleen, respectively. The fraction of the dose localized in other tissues was significantly lower than that localized in liver and spleen. MHSN could be excreted from the body even single administrated at high dose and the entire clearance of the particles required longer than 4 weeks (Fig. 11).

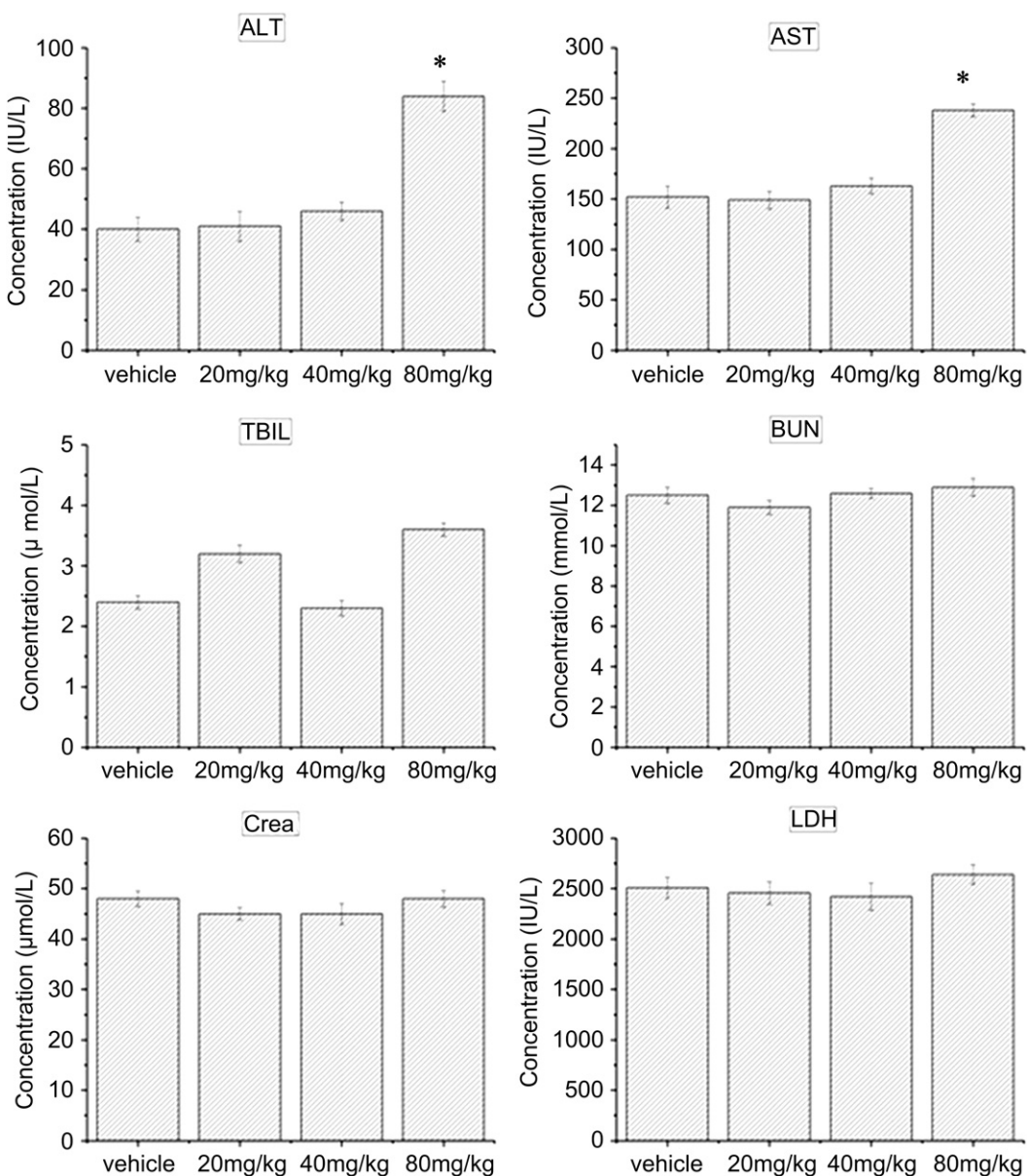


Fig. 9. Clinical Chemistry indexes of ICR mice following injection of MHSN by continuous intravenous injection. Mean and standard deviation of AST (a), ALT (b), TBIL(c), BUN(d), CREA (e), and LDH(f) of ICR mice ($n = 10$ per group). The serum ALT and AST level of the 160 mg/kg MHSN groups increased significantly ($p < 0.05$) comparing with control. (*denotes statistical significance for the comparison of control, $*p < 0.05$).

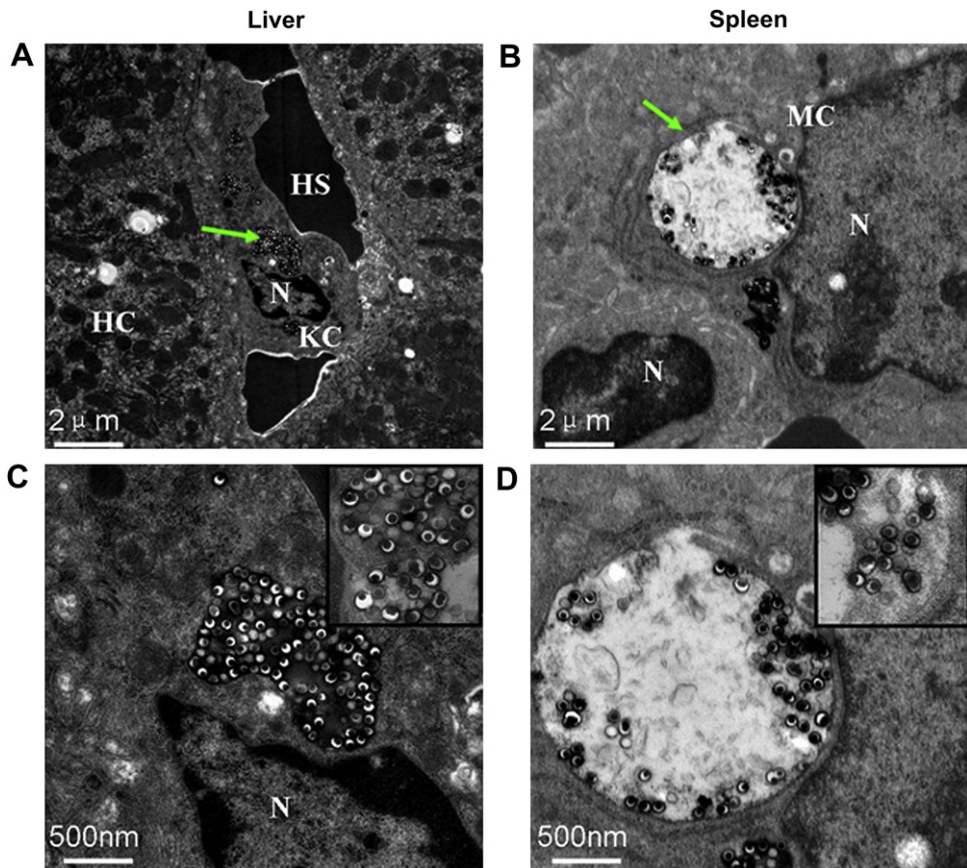


Fig. 10. TEM images of mice liver (A, C) and spleen (B, D) sacrificed 24 h post-injection with MHSN. The 2 μ m scale bar in a (6k), b (8k) panels, while the 500 nm scale bar applies to, c (30k), d (30k) panels. The lower row panels were magnifications of the regions indicated by green arrows in the upper row panels. N: nucleolus, HS: hepatic sinusoid, HC: hepatic cell, MC: macrophage cell, KC: Kupffer cells.

4. Discussion

The toxicity of carriers is a critical factor in evaluating the potential of new drug-delivery systems. However, there are no harmonized standards for assessing toxicity of nanoparticles after they enter the blood stream. Nanotoxicology is emerging as an important subdiscipline of nanotechnology, but it still being a question of nanomaterials safety evaluation. In the toxicological evaluation system, single dose toxicity and repeated dose toxicity are two general components. The general toxicity of compounds could be understood after these two evaluations. Repeated dose

toxicity refers to the harmful effects of long-term exposure to relatively low doses of toxicant. A single compound may generate both acute and chronic toxic effects depending on the dose and duration of exposure. Current knowledge of silica induced repeated dose toxicity is still incomplete.

In this paper, we examined MHSN single dose and repeated dose toxicity in mice. For the lethal toxicity, the LD₅₀ of MHSNs was greater than 1000 mg/kg, while repeated administration, 80 mg/kg continuous injection for 14 days would not result death. Hudson et al. reported that MCM-41 induced mice death in 15 min after intravenous administrations at 6 mg per animal (corresponding to 240 mg/kg) [23]. Hikaru et al. reported that intravenous injection of silica particles with diameters of 70 nm at 50 and 100 mg/kg was often lethal [24]. The present study provided clear evidence that LD₅₀ of MHSN with a size of 110 nm in mice was over 1000 mg/kg. In toxicology, dose is everything. However, the question of the most appropriate dose metric for nanoparticles has been debated [25]. A prevailing view in the field of nanotoxicology is that surface area is an important determinant of toxicity. The state of dispersion of nanoparticles is also important for nanotoxicological studies [26,27]. The results of single and repeated dose toxicity of MHSNs demonstrated low toxicity of the new nanostructure *in vivo*. Moreover, further studies of the relationship between toxicity and sizes, shapes or chemical modification on the surface of particles is needed.

For the non-lethal toxicity, no toxicity was found in liver, spleen, lung and kidney in MHSNs-injected mice at 40 and 160 mg/kg single dose and there were no abnormalities in the spleen, kidney and lung in MHSNs-injected mice at 500 and 1280 mg/kg. However,

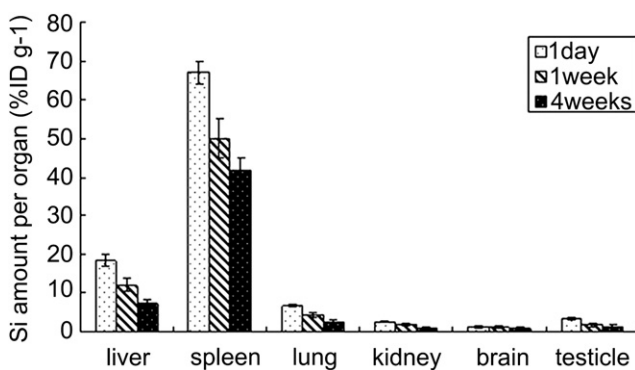


Fig. 11. ICP–OES analysis result of silicon levels in liver, spleen, lung, kidney and brain of animals treated with MHSNs.

lymphocytic infiltration, microgranulation and degenerative necrosis of hepatocytes were observed in the liver at 500 and 1280 mg/kg single administration. These results directly indicate that MHSN has low single dose toxicity and is great potential to use for drug delivery and imaging tools in live animals. For multiple doses, 20 mg/kg for 14 days continuous administrations would not cause abnormalities of any organs like liver, spleen and kidney. But high than 40 mg/kg dose, MHSNs could cause liver lesions. These findings will be useful for future development of nanotechnology-based drug delivery system and other biomedical applications.

Macrophages are described to have a predisposition for rapid recognition and clearance of particulate matter, and are therefore, well recognized as great nanocarrier targets [28]. Resident macrophages in the liver, Kupffer cells, play a pivotal role in defense against foreign particles by eliminating the particles via phagocytosis. The macrophage is a specialized host defense cell found in the reticuloendothelial system. Clearance and opsonization occur under certain conditions for nanoparticles depending on size and surface characteristics [29]. This means that differential opsonization translates into differences in clearance rates and macrophage sequestration of nanoparticles [30]. In this study, MHSNs were found to be distributed in the liver and spleen after 24 h intravenous injection. ICP–OES, fluorescent and ultrastructure localization of MHSN particles in liver and spleen confirmed that macrophage resident in liver and spleen was the target cell of MHSNs. Several reviews suggested that silica nanoparticles were degradable over time in the body [31–33]. We found that about 50% of MHSN was removed from the body over 4 weeks after injection. These particles would be excreted from the body and the entire clearance time of the particles should be over 4 weeks. The long circulation time of MHSN provided the possibility of controlled release drug carrier application *in vivo*.

5. Conclusion

In this paper, systematic single and repeated dose toxicity evaluation was carried out for MHSNs in mice. Mortality, clinical features, pathological examinations and blood biochemical indexes revealed low *in vivo* toxicity of MHSNs. The particles accumulated mainly in mononuclear phagocytic cells in liver or spleen and could excrete from the body exceed 4 weeks. Although liver injury caused by MHSNs at high dose were observed and more extensive series and long-term toxicity were needed to confirm this results, they do encourage further exploration of MHSNs in biomedical applications in living animals. And the fate, kinetics, clearance, metabolism, protein coating, immune response and toxicity of nanostructures to the nanostructure's physical properties are still not fully understood. Further evaluation of the relationship between toxicity and sizes, shapes or chemical modification on the surface of particles is needed, and the future studies based on these data will provide very useful information for future development of drug delivery system using nano-size materials.

Acknowledgment

The authors acknowledge financial support from the National Hi-Technology Research and Development Program (863 Program) (2007AA021803 and 2009AA03z322), the National Natural Science Foundation of China (NSFC) (No. 30800258, No.20873171, No. 30900349 and No. 60736001).

Appendix

Figure with essential color discrimination. Figs. 3, 6–10 in this article is difficult to interpret in black and white. The full color

images can be found in the online version, at doi:10.1016/j.biomaterials.2010.10.035.

Appendix. Supplementary data

Supplementary data related to this article can be found online at doi:10.1016/j.biomaterials.2010.10.035.

References

- Vega-Villa KR, Takemoto JK, Yanez JA, Remsberg CM, Forrest ML, Davies NM. Clinical toxicities of nanocarrier systems. *Adv Drug Deliv Rev* 2008;60(8):929–38.
- Aillon KL, Xie Y, El-Gendy N, Berkland CJ, Forrest ML. Effects of nanomaterial physicochemical properties on *in vivo* toxicity. *Adv Drug Deliv Rev* 2009;61(6):457–66.
- Fischer HC, Chan WC. Nanotoxicity: the growing need for *in vivo* study. *Curr Opin Biotechnol* 2007;18(6):565–71.
- Huang X, Zhuang J, Teng X, Li L, Chen D, Yan X, et al. The promotion of human malignant melanoma growth by mesoporous silica nanoparticles through decreased reactive oxygen species. *Biomaterials* 2010;31(24):6142–53.
- Chen AM, Zhang M, Wei D, Stueber D, Taratula O, Minko T, et al. Co-delivery of doxorubicin and Bcl-2 siRNA by mesoporous silica nanoparticles enhances the efficacy of chemotherapy in multidrug-resistant cancer cells. *Small* 2009;5(23):2673–7.
- Thomas MJ, Slipper I, Walunj A, Jain A, Favretto ME, Kallinteri P, et al. Inclusion of poorly soluble drugs in highly ordered mesoporous silica nanoparticles. *Int J Pharm* 2009;387(1–2):272–7.
- Vivero-Escoto JL, Slowing LL, Wu CW, Lin VS. Photoinduced intracellular controlled release drug delivery in human cells by gold-capped mesoporous silica nanosphere. *J Am Chem Soc* 2009;131(10):3462–3.
- Huang X, Teng X, Chen D, Tang F, He J. The effect of the shape of mesoporous silica nanoparticles on cellular uptake and cell function. *Biomaterials* 2010;31(3):438–48.
- Zhu Y, Shi J, Shen W, Dong X, Feng J, Ruan M, et al. Stimuli-responsive controlled drug release from a hollow mesoporous silica sphere/polyelectrolyte multilayer core-shell structure. *Angew Chem Int Ed Engl* 2005;44(32):5083–7.
- Chen Y, Chen H, Guo L, He Q, Chen F, Zhou J, et al. Hollow/rattle-type mesoporous nanostructures by a structural difference-based selective etching strategy. *ACS Nano* 2010;4(1):529–39.
- Zhu Y, Ikoma T, Hanagata N, Kaskel S. Rattle-type Fe(3)O(4)@SiO(2) hollow mesoporous spheres as carriers for drug delivery. *Small* 2010;6(3):471–8.
- Chen D, Li L, Tang F, Qi S. Facile and scalable synthesis of tailored silica nanorattle structures. *Adv Mater* 2009;21:3804–7.
- Slowing LL, Wu CW, Vivero-Escoto JL, Lin VS. Mesoporous silica nanoparticles for reducing hemolytic activity towards mammalian red blood cells. *Small* 2009;5(1):57–62.
- Low SP, Voelcker NH, Canham LT, Williams KA. The biocompatibility of porous silicon in tissues of the eye. *Biomaterials* 2009;30(15):2873–80.
- Tao Z, Morrow MP, Asefa T, Sharma KK, Duncan C, Anan C, et al. Mesoporous silica nanoparticles inhibit cellular respiration. *Nano Lett* 2008;8(5):1517–26.
- Zhu J, Tang J, Zhao L, Zhou X, Wang Y, Yu C. Ultrasmall, well-dispersed, hollow siliceous spheres with enhanced endocytosis properties. *Small* 2010;6(2):276–82.
- Radu DR, Lai CY, Jeftinija K, Rowe EW, Jeftinija S, Lin VS. A polyamidoamine dendrimer-capped mesoporous silica nanosphere-based gene transfection reagent. *J Am Chem Soc* 2004;126(41):13216–7.
- Slowing LL, Trewyn BG, Lin VS. Effect of surface functionalization of MCM-41-type mesoporous silica nanoparticles on the endocytosis by human cancer cells. *J Am Chem Soc* 2006;128(46):14792–3.
- Liu Y, Miyoshi H, Nakamura M. Novel drug delivery system of hollow mesoporous silica nanocapsules with thin shells: preparation and fluorescein isothiocyanate (FITC) release kinetics. *Colloids Surf B Biointerfaces* 2007;58(2):180–7.
- Hamilton Jr RF, Thakur SA, Holian A. Silica binding and toxicity in alveolar macrophages. *Free Radic Biol Med* 2008;44(7):1246–58.
- Sayes CM, Reed KL, Glover KP, Swain KA, Ostraat ML, Donner EM, et al. Changing the dose metric for inhalation toxicity studies: short-term study in rats with engineered aerosolized amorphous silica nanoparticles. *Inhal Toxicol* 2010;22(4):348–54.
- Arts JH, Muijsen H, Duistermaat E, Junker K, Kuper CF. Five-day inhalation toxicity study of three types of synthetic amorphous silicas in Wistar rats and post-exposure evaluations for up to 3 months. *Food Chem Toxicol* 2007;45(10):1856–67.
- Hudson SP, Padera RF, Langer R, Kohane DS. The biocompatibility of mesoporous silicates. *Biomaterials* 2008;29(30):4045–55.
- Nishimori Hikaru, Kondoh Masuo, Isoda Katsuhiro, Tsunoda Shin-ichi, Tsutsumi Yasuo, Yagi Kiyohito. Silica nanoparticles as hepatotoxins. *Eur J Pharm Biopharm* 2009;72:496–501.
- Oberdorster G, Oberdorster E, Oberdorster J. Concepts of nanoparticle dose metric and response metric. *Environ Health Perspect* 2007;115(6):A290.

- [26] Lanone S, Boczkowski J. Biomedical applications and potential health risks of nanomaterials: molecular mechanisms. *Curr Mol Med* 2006;6(6):651–63.
- [27] Oberdorster G, Oberdorster E, Oberdorster J. Nanotoxicology: an emerging discipline evolving from studies of ultrafine particles. *Environ Health Perspect* 2005;113(7):823–39.
- [28] Garnett MC, Kallinteri P. Nanomedicines and nanotoxicology: some physiological principles. *Occup Med (Lond)* 2006;56(5):307–11.
- [29] Curtis J, Greenberg M, Kester J, Phillips S, Krieger G. Nanotechnology and nanotoxicology: a primer for clinicians. *Toxicol Rev* 2006;25(4):245–60.
- [30] Moghimi SM, Hunter AC, Murray JC. Nanomedicine: current status and future prospects. *FASEB J* 2005;19(3):311–30.
- [31] Radin S, El-Bassyouni G, Vresilovic EJ, Schepers E, Ducheyne P. In vivo tissue response to resorbable silica xerogels as controlled-release materials. *Biomaterials* 2005;26(9):1043–52.
- [32] Roy I, Ohulchansky TY, Pudavar HE, Bergey EJ, Oseroff AR, Morgan J, et al. Ceramic-based nanoparticles entrapping water-insoluble photosensitizing anticancer drugs: a novel drug-carrier system for photodynamic therapy. *J Am Chem Soc* 2003;125(26):7860–5.
- [33] Li X, Shi J, Zhu Y, Shen W, Li H, Liang J, et al. A template route to the preparation of mesoporous amorphous calcium silicate with high in vitro bone-forming bioactivity. *J Biomed Mater Res B Appl Biomater* 2007; 83(2):431–9.